

Published in final edited form as:

J Membr Biol. 2006 ; 213(1): 19–29. doi:10.1007/s00232-006-0037-y.

## Functional expression of inward rectifier potassium channels in cultured human pulmonary smooth muscle cells:

evidence for a major role of Kir2.4 subunits

Brian P. Tennant<sup>#</sup>, Yi Cui<sup>#</sup>, Andrew Tinker, and Lucie H. Clapp<sup>\*</sup>

BHF Laboratories, Department of Medicine, Rayne Institute, University College London 5 University Street, London, WC1E 6JF

### Abstract

Strong inwardly rectifying K<sup>+</sup> (K<sub>IR</sub>) channels that contribute to maintaining the resting membrane potential are encoded by the Kir2.0 family (Kir2.1-2.4). In smooth muscle, K<sub>IR</sub> currents reported so far have the characteristics of Kir2.1. However, Kir2.4, which exhibits unique characteristics of barium block, has been largely overlooked. Using patch-clamp techniques, we characterized K<sub>IR</sub> channels in cultured human pulmonary artery smooth muscle (HPASM) cells and compared to cloned Kir2.1 and Kir2.4 channels. In a physiological K<sup>+</sup> gradient, inwardly rectifying currents were observed in HPASM cells, the magnitude and reversal potential of which were sensitive to extracellular K<sup>+</sup> concentration. Ba<sup>2+</sup> (100 μM) significantly inhibited inward currents and depolarised HPASM cells by ~10 mV. In 60 mM extracellular K<sup>+</sup>, Ba<sup>2+</sup> blocked K<sub>IR</sub> currents in HPASM cells with IC<sub>50</sub> of 39.1 μM at -100 mV, compared to 3.9 μM and 65.6 μM for Kir2.1 and Kir2.4, respectively. Cloned Kir2.4 and K<sub>IR</sub> currents in HPASM cells showed little voltage dependence to Ba<sup>2+</sup> inhibition, which blocked at a more superficial site than for Kir2.1. Single channel recordings revealed strong inwardly rectifying channels with an average conductance of 21 pS in HPASM cells, not significantly different from either Kir2.1 (19.6 pS) or Kir2.4 (19.4 pS). RT-PCR detected products corresponding to Kir2.1, Kir2.2 and Kir2.4 but not Kir2.3. We demonstrate that cultured HPASM cells express K<sub>IR</sub> channels and suggest both Kir2.1 and Kir2.4 subunits contribute to these channels, although the whole-cell current characteristics described, share more similarity with Kir2.4.

### Keywords

Inward rectifier potassium channels; pulmonary artery; human; Kir2.4; patch-clamp

### INTRODUCTION

Strong inwardly rectifying K<sup>+</sup> (K<sub>IR</sub>) channels have been described in many vascular and visceral tissues from different species (Quayle *et al.*, 1997; Nilius & Droogmans, 2001). These channels pass most current at potentials hyperpolarised to the K<sup>+</sup> equilibrium potential (E<sub>K</sub>), though the small amount of outward current carried at voltages depolarised to this potential, is enough to regulate the resting membrane potential (E<sub>m</sub>) and to cause blood vessel dilatation in response to either raised extracellular (10–15 mM) K<sup>+</sup> (Quayle *et al.*, 1997) or shear stress (Hoger *et al.*, 2002). Since their initial identification in rat cerebral and coronary artery (Edwards *et al.*, 1988; Quayle *et al.*, 1993; Knot *et al.*, 1996), patch-clamp

<sup>\*</sup> Author for Correspondence, BHF Laboratories, Department of Medicine, 4<sup>th</sup> Floor Rayne Institute, University College, 5 University Street, London WC1E 6JJ, Tel 020 7679 6180, Fax 020 7679 6205, Email l.clapp@ucl.ac.uk.

<sup>#</sup> Authors contributed equally to the work

studies have reported strongly rectifying inward currents in isolated lung endothelial and bronchial smooth muscle cells (Voets *et al.*, 1996; Kamouchi *et al.*, 1997; Snetkov & Ward, 1999; Michelakis *et al.*, 2001; Hogg *et al.*, 2002; Oonuma *et al.*, 2002; Shimoda *et al.*, 2002). Regardless of their origin within the cardiovascular system,  $K_{IR}$  currents recorded to date are potently blocked by micromolar external  $Ba^{2+}$  ions in a manner that is steeply voltage and time-dependent (Quayle *et al.*, 1993; Robertson *et al.*, 1996; Bradley *et al.*, 1999; Snetkov & Ward, 1999; Sakai *et al.*, 2002; Oonuma *et al.*, 2002).

At the molecular level, the Kir2.0 subfamily almost certainly encode the classical inward rectifiers found in the brain, heart, skeletal and vascular muscle (Quayle *et al.*, 1997; Stanfield *et al.*, 2002). These channels form as tetramers of subunits that have only two membrane-spanning regions between which is the H5 loop responsible for potassium selectivity. Four isoforms have been identified, Kir2.1, 2.2, 2.3 and 2.4 (Stanfield *et al.*, 2002). The properties of the first three have been extensively characterised, while that of Kir2.4, has been much less studied, probably due to its restricted expression. Apart from Kir2.4 all subunits show the blueprint of voltage and time-dependent block with  $Ba^{2+}$  (Bradley *et al.*, 1999; Hughes *et al.*, 2000; Preisig-Muller *et al.*, 2002; Schram *et al.*, 2002). In smooth muscle the evidence so far indicates that Kir2.1 might encode  $K_{IR}$  currents both in native and cultured smooth muscle cells. The RT-PCR analysis demonstrated the presence of Kir2.1 but not Kir2.2 and Kir2.3 in rat cerebral, coronary and mesenteric artery, canine colonic smooth muscle, and human bronchial smooth muscle (Bradley *et al.*, 1999; Oonuma *et al.*, 2002; Flynn *et al.*, 1999), although Kir2.4 was not examined in these studies. Moreover, expression of Kir2.1 cloned from rat mesenteric vascular smooth muscle cells into *Xenopus* oocytes produced  $K_{IR}$  currents that resembled those observed in native vascular smooth muscle cells (Bradley *et al.*, 1999).

The aim of the present study was to identify and examine the properties of  $K_{IR}$  channels in cultured human pulmonary artery smooth muscle (HPASM) cells and determine the expression of members of Kir2.0 subfamily. Here we show that three out of the four Kir2.0 subunits are expressed at the transcriptional level in cultured HPASM cells and that the properties of the  $K_{IR}$  currents recorded in these cells most closely resembles that of Kir2.4, although other subunits are likely to contribute. We thus provide the first functional evidence for a role of Kir2.4 outside the central and peripheral nervous system.

## MATERIALS AND METHODS

### Cell culture

Cultured HPASM cells were obtained from Clonetics (4<sup>th</sup> passage) and plated in smooth muscle growth medium (SmGM, Clonetics, USA) supplemented with gentamicin (50  $\mu$ g/ml), human epidermal (0.5  $\mu$ g/ml) and fibroblast growth factors (1.0  $\mu$ g/ml), insulin (5  $\mu$ g/ml) and 5% foetal bovine serum. Cells were grown at 37 °C in humidified atmosphere of 5%  $CO_2$  as described (Cui *et al.*, 2002). After reaching confluence, cells were scratched from the dish by treatment with accutase (JCS Biologicals) and transferred to T75 flasks for further passage. Smooth muscle cells were characterized by immunohistochemical staining using a mouse anti  $\alpha$ -actin monoclonal antibody (Boehringer, Germany). For electrophysiological experiments, cells (up to 8<sup>th</sup> passage) were plated onto cover slips in six well plates at a density of 30,000 cells/well and at 24 hr the growth medium was replaced by serum-free Dulbecco's Modified Eagle's Medium (DMEM, without antibiotics) to inhibit cell proliferation. Experiments were performed on cells starved of serum for at least 24 hours. HEK-293 cells (human embryonic kidney cell line) were cultured under a humidified atmosphere in 5%  $CO_2$  in minimal essential medium supplemented with Earle's Salts, L-glutamine 10%, foetal bovine serum 10 %, 1% penicillin/streptomycin (from a stock of 10,000 units/ml penicillin and 1 mg/ml streptomycin).

## Transfection and generation of monoclonal stable lines

Mouse Kir2.1 cDNA was a kind gift from Lilly Jan (Howard Hughes Medical Institute, University of California, CA) and rat Kir2.4 cDNA was a kind gift from Diomedes Logothetis (Mount Sinai School of Medicine, New York). HEK-293 cells were transfected with Kir2.1 and Kir2.4 subcloned into in pcDNA3 vectors (Invitrogen) using LipofectAMINE (Life Technologies, Inc) according to the manufacturer's instructions (Cui *et al.*, 2001). Stable cell lines were established using the appropriate antibiotic selection (G418, for Kir2.1; Zeocin for Kir2.4) as detailed previously (Giblin *et al.*, 1999). In some experiments HEK-293 cells were transiently transfected with Kir2.1 and GFP cDNAs and successfully transfected cells identified by epifluorescence.

## Molecular Biology

To identify  $K_{IR}$  channels in HPASM cells by molecular methods, RT-PCR was used. For messenger RNA isolation, HPASM cells were grown in  $3 \times T175$  flasks to confluence and washed twice with cold PBS (made in DEPC  $H_2O$ ). Using an RNA isolation kit (Fast-track2.0, Invitrogen) and following the manufacturer instructions, polyA RNA was isolated using the oligo dT cellulose column provided. Synthesis of cDNA was carried out using  $1 \mu\text{l}$  polyA RNA (100 ng) and oligo dT primers and following the manufacturer's instructions (cDNA cycle kit, Invitrogen). For PCR,  $2 \mu\text{l}$  of cDNA was used in a  $50 \mu\text{l}$  reaction and the following added:  $5 \mu\text{l}$  PCR buffer ( $\times 10$ , containing  $1.5 \text{ mM MgCl}_2$ ) (Boehringer Mannheim),  $1 \mu\text{l}$  deoxynucleoside-5'-triphosphate solution (containing  $25 \text{ mM}$  of each dNTP), 1 unit Taq DNA polymerase (Boehringer Mannheim) and  $1 \mu\text{M}$  of each specific primers. Primers: Kir2.1 (GenBank accession no AF153819) forward (5'-TCTTGGGAATTCTGGTTTGC-3'), Kir2.1 reverse (5'-TGGGAGCCTTGTGGTTCTAC-3'), Kir2.2 (NM\_021012) forward (5'-TCGATGTGGGCTTCGACAA-3'), Kir2.2 reverse (5'-GTAGAGGGCACCTCATAGG-3'), Kir2.3 (U07364) forward (5'-AACCGCTTCGTCAGAAGAA-3'), reverse (5'-GATACACCAGAAGAGGAGGC-3'), Kir2.4 (AF081466) forward (5'-AATGGGGTGGAAACAGAAGATG-3'), reverse (5'-GTCTATACCATTGGCTTCTCAC-3'). The cycling conditions were  $94 \text{ }^\circ\text{C}$  for 30 s,  $54 \text{ }^\circ\text{C}$  for 30 s,  $74 \text{ }^\circ\text{C}$  for 30 s, for 35 cycles and final extension 10 min. As a negative control,  $2 \mu\text{l}$  of the RT-PCR product synthesised in the absence of AMV-Transcriptase was used as a template. PCR products were electrophoresed on a 1.3 % agarose gel. The sequence of PCR products was confirmed by sequencing using a dye terminator kit (Applied Biosciences) and an automatic sequencer (ABI377, Perkin-Elmer). As a positive control for Kir2.3, human Kir2.3 cDNA (Gene Service, Cambridge, UK) was amplified under the same conditions, using only  $12.5 \text{ pg}$  of cDNA as template.

## Electrophysiological recording

Currents and membrane potentials were recorded in the whole-cell and cell-attached configuration of the patch-clamp technique using an Axopatch 200B amplifier (Axon Instruments, Foster City, CA). Current signals were filtered at  $1\text{-}2 \text{ kHz}$  (8-pole low-pass Bessel) and digitised at  $5 \text{ kHz}$  using Digidata 1200 interface and saved onto computer for later analysis. Patch pipettes from either thin ( $1.7 \text{ mm O.D}$ ) or thick walled ( $1.5 \text{ mm O.D}$ ) borosilicate glass capillaries (Clark Electromedical, Pangbourne, UK) were pulled and fire polished using a DMZ-universal puller (Zietz Instruments, Germany). Pipettes had resistances of  $2\text{-}4 \text{ M}\Omega$  for whole-cell recordings and  $6\text{-}12 \text{ M}\Omega$  for single channel recordings when filled with electrolyte solution. Electrode capacitance was reduced by coating pipettes with a parafilm/mineral oil suspension and compensated electronically. Series resistance during whole-cell recording was compensated to at least 75% by the amplifier.

## Data analysis

Electrophysiological data were analysed using pClamp (version 6, Axon Instruments), SATORI v3.2 (Intracel, Coventry, U.K.) and Origin software (version 6 & 7; Microcal Software, Northampton, MA, USA). Values are given as means  $\pm$  S.E.M. and *n* indicates the number of cells. For current-voltage (I-V) relationship graphs, current was measured during the final 10 ms of each voltage step and averaged for each cell. The barium concentration-response curves were analysed and fitted using the sigmoidal fitting routine in Origin. The drug concentration at which half-maximum current is inhibited ( $K_D$ ) was obtained using the Logistical function (Eq 1)

$$\frac{I_{Ba}}{I_{Con}} = \frac{1}{1+(X/K_D)^n} \quad (1)$$

where  $I_{Ba}$  is the current in the presence of barium,  $I_{Con}$  is the current in control,  $X$  is the extracellular  $Ba^{2+}$  concentration and  $n$  is the slope factor (Hill coefficient). Statistical significance was assessed using a paired or unpaired Student's *t*-test. *P* values  $<0.05$  were considered to be statistically significant.

## Solutions and drugs

For whole-cell recordings in HPASM cells, the standard bath solution was an extracellular physiological salt solution (PSS) containing (mM): 137 NaCl, 5 KCl, 0.4  $KH_2PO_4$ , 0.3  $NaH_2PO_4$ , 2  $NaHCO_3$ , 1  $MgCl_2$ , 1.8  $CaCl_2$ , 10 HEPES and 5.5 glucose (pH 7.4 with NaOH). To assess the voltage-dependence of  $Ba^{2+}$  block and the effect on the reversal potential, whole-cell experiments in HPASM and HEK-293 cells were conducted in a high potassium bath solution (60 mM  $K^+$ ), which was made by replacing NaCl in the PSS with an equimolar concentration of KCl. The basic pipette solution contained (mM): 130 KCl, 1  $MgCl_2$ , 1 EGTA, 15 HEPES, 1 Adenosine triphosphate- $Na_2$  (ATP). The pH of the solutions was adjusted to 7.20 with KOH, to give a final  $K^+$  concentration of 140 mM. For single channel recordings, the pipette and bath solution was (mM): 140 KCl, 1.0  $MgCl_2$ , 1 EGTA, 10 HEPES (pH 7.2 NaOH).  $BaCl_2$ , adenosine triphosphate- $Na_2$  (ATP) and glibenclamide were obtained from Sigma Chemical Co. (Poole, Dorset, UK).

## RESULTS

### Whole-cell inward rectifier currents in physiological $K^+$ and high (60 mM) $K^+$ gradient

Cultured HPASM cells were perfused with a physiological salt solution containing 5 mM  $K^+$  and dialyzed with a pipette solution containing 140 mM  $K^+$ . Under these conditions, application of 300 ms voltage steps from  $-150$  mV to  $+40$  mV at a holding potential of  $-60$  mV, evoked both inward and outward currents (Figure 1A). Upon application of the  $K_{IR}$  channel blocker,  $Ba^{2+}$  (100  $\mu$ M), only currents activated in the inward direction were significantly inhibited (Figure 1A, lower panel). Figure 1B shows mean current-voltage (I-V) relationships of currents obtained from experiments similar to that shown in figure 1A. Inward currents measured at  $-120$  mV were reduced by 70% from  $-66.3 \pm 10.7$  pA under control conditions to  $-19.4 \pm 3.21$  pA ( $n=8$ ,  $P<0.01$ ) in the presence of  $Ba^{2+}$ . Such effects were fully reversible upon washout of  $Ba^{2+}$  (Figure 1B). In contrast, outward currents evoked by voltages positive to  $-30$  mV were essentially unaffected by the same concentration of  $Ba^{2+}$  (Figure 1B), such that currents measured at  $+40$  mV were  $56.9 \pm 10.6$  pA under control conditions and  $62.8 \pm 6.8$  pA ( $P>0.05$   $n=8$ ) in the presence of  $Ba^{2+}$ . Plotting the  $Ba^{2+}$ -sensitive current revealed the characteristics of inward rectification of the current, having a reversal potential of  $-74.4 \pm 2.2$  mV ( $n=8$ ) in a 5/140 mM  $K^+$  gradient (Figure 1C). This is close to the calculated  $E_K$  under these conditions of  $-82$  mV. Since  $K_{IR}$  channels are highly selective for  $K^+$  ions, showing a positive shift in the I-V relationship and

an increase in conductance of the channel with increasing concentration of extracellular  $K^+$ , we further characterized currents by performing experiments with 60 mM  $K^+$  in the bathing solution. Under these conditions, the same voltage clamp protocols as above were applied. As expected, bigger inward currents were evoked at hyperpolarized potentials averaging  $-378.0 \pm 78.4$  pA at  $-120$  mV ( $n=6$ ). Upon application of  $Ba^{2+}$  (30  $\mu$ M) currents were significantly inhibited to  $-232.1 \pm 41.5$  pA ( $P < 0.01$ ,  $n=6$ ). The mean IV relationship of the  $Ba^{2+}$ -sensitive current is shown in figure 1C, giving a reversal potential of  $-22.4 \pm 3.0$  mV ( $n=11$ ) for the current, close to the calculated  $E_K$  of  $-21$  mV under these conditions. Similarly, outward currents were not affected ( $360.6 \pm 72.8$  pA at  $+40$  mV under control conditions and  $381.8 \pm 77.7$  pA in the presence of  $Ba^{2+}$ ,  $P > 0.05$ ,  $n=6$ ). In addition, the  $K_{ATP}$  channel blocker, glibenclamide (10  $\mu$ M) had no effect on the  $Ba^{2+}$ -sensitive currents (data not shown). Thus the  $Ba^{2+}$ -sensitive current shifted when  $K^+$  was altered and reversed near the expected  $E_K$  indicating that currents were indeed through  $K^+$ -selective channels.  $K_{IR}$  channels have been proposed to contribute to the maintenance of resting membrane potential, so their potential role was examined in current clamp ( $I=0$  mode) in cells bathed in a physiological salt solution. Under these conditions, cells had a resting potential of  $-44.3 \pm 4.4$  mV ( $n=7$ ). Following application of 100  $\mu$ M  $Ba^{2+}$ , the resting potential became significantly more depolarised to  $-34.7 \pm 3.0$  mV ( $P < 0.05$  paired t-test). These results indicate that  $K_{IR}$  currents contribute to the maintenance of resting membrane potential in cultured HPASM cells.

### Characteristics of $Ba^{2+}$ block in HPASM

To determine the nature of the  $Ba^{2+}$  block, inhibition of the current was examined over a range of  $Ba^{2+}$  concentrations (1-1000  $\mu$ M) in the presence of 60 mM extracellular  $K^+$ . Figure 2A shows families of inward currents activated by 300 ms pulses from  $-150$  to 0 mV in an increment of 10 mV. In this and most cells, inward currents were typically noisy at membrane potentials at or below  $-80$  mV. Application of  $Ba^{2+}$  blocked inward current above a concentration of 1  $\mu$ M, though block showed little or no time dependency in this or any other HPASM cell, but it did reduce current noise seen at negative potentials. Figure 2B summarises results of experiments from nine HPASM cells where the average steady-state I-V relationship in presence of increasing concentrations of  $Ba^{2+}$  has been plotted. The concentration-dependence of the  $Ba^{2+}$  block was assessed by plotting mean values of the fractional current remaining in the presence of  $Ba^{2+}$ . Using nonlinear least squares optimisation and fitting data to Eq 1, the extrapolated value for the  $K_D$  at  $-100$  mV was 39.1  $\mu$ M (Figure 2C), although it should be noted that the hill-coefficient of the sigmoidal fit was shallow (slope = 0.37). One possible explanation is that whole-cell current contains at least 2 populations of  $K_{IR}$  channels with distinct  $Ba^{2+}$  sensitivities. Amongst the Kir2.0 family,  $Ba^{2+}$  block is most sensitive in Kir2.2, followed by 2.1, 2.3 and 2.4, with the  $IC_{50}$  being  $\sim 0.5$   $\mu$ M, 3.2  $\mu$ M, 10-18  $\mu$ M and 70-116  $\mu$ M, respectively (Topert *et al.*, 1998; Hughes *et al.*, 2000; Liu *et al.*, 2001; Preisig-Muller *et al.*, 2002; Schram *et al.*, 2002). Thus based on the characteristics of the  $Ba^{2+}$  block of  $K_{IR}$  currents in cultured HPASM cells would suggest a major contribution from Kir2.4. We therefore sought to make comparisons with Kir2.1 and Kir2.4 subunits stably expressed in HEK-293 cells.

### Comparisons of $Ba^{2+}$ block of Kir2.1 and Kir2.4 stably expressed in HEK-293 cells

The effect of  $Ba^{2+}$  (0.03-10000  $\mu$ M) was studied under similar experimental conditions to the above against currents activated in a 60/140K<sup>+</sup> gradient. In cells expressing Kir2.1,  $Ba^{2+}$  significantly blocked inward currents in a manner that was visibly time-dependent (Figure 3A), with little block of the instantaneous inward current at 10 or 100  $\mu$ M, but almost complete block of the steady-state current at the end of the voltage step. By comparison, currents carried by Kir2.4 were weakly affected by  $Ba^{2+}$  at 10  $\mu$ M, showed no time dependence to the block, and required mM  $Ba^{2+}$  to produce near full block in the inward



direction and partial (50%) in the outward direction. Figure 3B summarises the average steady-state I-V relationships for Kir2.1 and Kir2.4, where current for each subunit is plotted relative to that activated at  $-150$  mV. The I-V relationships show a similar profile of steep inward rectification although Kir2.4 passes significantly ( $P < 0.05$ ,  $n = 6-12$ ) more outward current at positive potentials, whether this is given in absolute terms ( $150 \pm 34$  versus  $70 \pm 7$  pA) or relative to control current at  $-150$  mV ( $0.05 \pm 0.01$  versus  $0.01 \pm 0.001$ ) for the current measured at  $+20$  mV. As expected for a  $K^+$  current, the reversal potential of the current blocked by  $100 \mu\text{M Ba}^{2+}$  was  $18.6 \pm 2.8$  mV ( $n = 8$ ) and  $21.8 \pm 2.3$  mV ( $n = 7$ ) for Kir2.1 and Kir2.4, respectively. The concentration-dependence of the  $\text{Ba}^{2+}$  block for the two subunits was assessed by plotting mean values of fractional current and fitting the data to Eq. 1 (Figure 3C). Using this approach, gave  $K_D$  values at  $-100$  mV of  $3.9 \mu\text{M}$  and  $65.6 \mu\text{M}$  for Kir2.1 and Kir2.4, respectively.

### Voltage-dependence of the $\text{Ba}^{2+}$ block

The effect of membrane potential on the  $K_D$  of barium block was compared for Kir2.1 and Kir2.4. (Figure 4A). In cells expressing Kir2.1, the  $K_D$  increased  $\sim 10$  fold between that calculated at  $-100$  mV and at  $-40$  mV, as evidenced by the rightward shift in the dose-response curves. By contrast the  $K_D$  in Kir2.4 expressing cells showed much less dependence on voltage, increasing only 3 fold over the same voltage range. In HPASM cells, the effect of voltage appeared to be intermediate between Kir2.1 and Kir2.4, though at  $-60$  mV and above, the  $K_D$  became more steeply dependent on voltage (Figure 2C). The voltage-dependence of the block can be investigated by the quantitative approach used by Woodhull (Woodhull, 1973). The basic assumption is that there is a single site accessible to a blocker with a valence of  $z$ , lying at a fractional distance  $\delta$  into the transmembrane field. Data obtained from figure 2C and 4A were fitted to Eq. 2 where the ratio of the current in the presence of the blocker over the control current ( $I/I_{\text{Con}}$ ) is plotted as a function of voltage ( $V$ ) at a single blocker concentration  $[B]$  to extrapolate values for

$$\frac{I}{I_{\text{Con}}} = \frac{1}{1 + \{[B]/K_D(0)\} e^{z\delta(FV/RT)}} \quad (2)$$

$K_D(0)$ , the dissociation constant at 0 mV and  $\delta$ .  $F$ ,  $R$  and  $T$  have their usual meanings and  $RT/F$  is 25.2 mV at 20 °C. Using this approach, the best fit parameters at a blocking concentration of  $100 \mu\text{M Ba}^{2+}$  were  $K_D(0) = 142 \pm 23 \mu\text{M}$ ,  $197 \pm 18 \mu\text{M}$ ,  $337 \pm 45 \mu\text{M}$  and  $\delta = 0.38 \pm 0.04$ ,  $0.15 \pm 0.02$ ,  $0.21 \pm 0.03$ , for Kir2.1 ( $n = 10$ ), Kir2.4 ( $n = 9$ ) and HPASM ( $n = 9$ ) cells respectively (Figure 4B). The  $\delta$  value for Kir2.1 was significantly different from that of Kir2.4 and HPASM ( $P < 0.001$ ). Varying the  $\text{Ba}^{2+}$  concentration by 10 fold gave similar values for  $\delta$ , though this altered  $K_D(0)$  by 3-4 fold (see Figure 4 legend). These data suggest that  $\text{Ba}^{2+}$  appears to act at a more superficial site in HPASM cells than would be predicted if native  $K_{\text{IR}}$  channels were composed of just Kir2.1 subunits and values for  $K_D(0)$  and  $\delta$  are closer to that obtained for channels made up of cloned Kir2.4 subunits.

### Single channel recordings

The properties of the  $\text{Ba}^{2+}$ -sensitive currents in HPASM cells were investigated in the cell-attached configuration, and compared with HEK293 cells expressing cloned Kir2.1 or Kir2.4 channels. Recordings were made in symmetrical  $K^+$  ( $140/140$  mM). Additionally, we also made recordings of Kir2.4 in the presence of  $\text{Ba}^{2+}$  ( $300 \mu\text{M}$  in the patch pipette). This was done because the only report to date describing a conductance for Kir2.4, by single channel recordings (Topert *et al.*, 1998) used this approach to reduce channel open probability in their analysis. We wished to establish if  $\text{Ba}^{2+}$  has any effect on conductance. Figure 5A shows typical single channel recordings obtained over a range of potentials from  $-120$  mV to  $+60$  mV in each experimental condition. The channels all showed strong inward

rectification as indicated by an increase current with membrane hyperpolarisation and the lack of channel openings at positive potentials. All channels had a high open probability (Figure 5B) and this decreased for Kir2.4 in the presence of Ba<sup>2+</sup>. Similar recordings were obtained in around 20% of HPASM cells and for Kir2.1, single channel inward currents were observed at negative membrane potentials in nearly all patches. Kir2.4, due to its high open probability, was less easily identified, with resolvable channel openings being observed in less than 5% of cells patched. However, in the presence of Ba<sup>2+</sup> the success rate was similar to that of Kir2.1 and records had less background noise. Slope conductances were calculated from the I-V relationships (Figure 5C) and gave average conductances of  $20.9 \pm 0.7$  pS (n=6),  $19.6 \pm 0.5$  pS (n=7) and  $19.4 \pm 1.7$  pS (n=4), for HPASM, Kir2.1 and Kir2.4, respectively. For Kir2.4 in the presence of Ba<sup>2+</sup>, a slope conductance of  $22.1 \pm 0.9$  pS (n=4) was obtained, which was not significantly different from in the absence of Ba<sup>2+</sup>. With such similar conductances for all the K<sub>IR</sub> channels tested, it appears not possible to dissect the molecular components of K<sub>IR</sub> currents in HPASM cells on the basis of single channel conductance alone. It should also be noted that inward rectifier channels having conductances between 7 pS and 35 pS, were occasionally observed in HPASM cells, and these may represent either subconductance levels of K<sub>IR</sub> channels or the existence of distinct populations of channels.

### RT-PCR analysis

RT-PCR analysis of Kir channels was carried out in cultured HPASM cells grown to confluence. PCR was performed in the presence of specific primers for Kir2.1, Kir2.2, Kir2.3 and Kir2.4. Reaction products corresponding to the expected fragment sizes for Kir2.1, Kir2.2 and Kir2.4 but not Kir2.3 were detected in the mRNA from cultured HPASM cells (Figure 6A). Similar results were obtained in another two experiments. Each of the positive PCR products was confirmed by DNA sequence analysis and found to be correct. A positive control for human Kir2.3 was used to confirm that the primer set used in HPASM cells did indeed give the predicted PCR band (Figure 6B).

## DISCUSSION

K<sub>IR</sub> channels are expressed in a variety of vascular and visceral smooth muscle tissues. The present study shows for first time that K<sub>IR</sub> channels also exist in cultured human pulmonary artery smooth muscle cells. This conclusion is based on the following major findings: (1) Inward currents showed strong inward rectification and were concentration-dependently blocked by Ba<sup>2+</sup>, with little effect of this agent on outward currents. (2) The reversal potential of Ba<sup>2+</sup>-sensitive currents was close to the expected E<sub>K</sub> and shifted when external K<sup>+</sup> concentration was altered. (3) RT-PCR analysis confirmed the existence of the Kir2.0 subfamily. (4) Single channel studies revealed K<sup>+</sup> channel currents with strong inward rectification.

### Biophysical properties of K<sub>IR</sub> currents

Within the lung, patch-clamp studies have reported inward currents with rectification strongly dependent on membrane potential and the K<sup>+</sup> gradient in isolated pulmonary artery and vein endothelial cells (Voets *et al.*, 1996; Kamouchi *et al.*, 1997; Michelakis *et al.*, 2001; Hogg *et al.*, 2002; Shimoda *et al.*, 2002), in human bronchial smooth muscle (Snetkov & Ward, 1999; Oonuma *et al.*, 2002) and in human lung cancer cells (Sakai *et al.*, 2002). Similar to that observed in other smooth muscles (Quayle *et al.*, 1997), block by barium is steeply voltage-dependent, increasing exponentially with hyperpolarisation and taking many milliseconds to develop (Snetkov & Ward, 1999; Sakai *et al.*, 2002; Oonuma *et al.*, 2002). Our results in cultured HPASM cells provide evidence for a K<sub>IR</sub> current with different characteristics to those previously described in the vasculature or in different types of

cultured human lung cells (Voets *et al.*, 1996; Snetkov & Ward, 1999; Sakai *et al.*, 2002; Oonuma *et al.*, 2002). For one, Ba<sup>2+</sup> block of inward currents showed little time- or voltage-dependence. This is consistent with Ba<sup>2+</sup> blocking at a more superficial site within the pore ( $\delta=0.21$ ) than has previously been described for native K<sub>IR</sub> currents in vascular smooth muscle (Quayle *et al.*, 1993; Robertson *et al.*, 1996). In these studies, the fraction of the applied electric field sensed by Ba<sup>2+</sup> was reported to be between 0.51 and 0.55. While we report a  $\delta$  value in our studies that is slightly lower for Kir2.1 (0.38), if measured using previous methods (K<sub>D</sub> values versus membrane potential), this approaches a similar value ( $\delta=0.48$ ; data not shown). The other thing to note was inward currents in HPASM were 10-30 fold less sensitive to Ba<sup>2+</sup> than we found for either cloned mouse Kir2.1 measured under similar conditions or previously reported for cloned rat Kir2.1 isolated from mesenteric artery (Bradley *et al.*, 1999). In native smooth muscle cells, K<sub>IR</sub> currents are even more sensitive to Ba<sup>2+</sup>, where the K<sub>D</sub> ranges from  $\sim 0.4 - 1 \mu\text{M}$  at  $-100 \text{ mV}$  (Quayle *et al.*, 1993; Oonuma *et al.*, 2002; Robertson *et al.*, 1996; Oonuma *et al.*, 2002). However, the sensitivity and characteristics of the Ba<sup>2+</sup> block shown here more closely resembled that of cloned Kir2.4, the only member of the Kir2.0 family to demonstrate a low Ba<sup>2+</sup> sensitivity and weak voltage-dependence (Hughes *et al.*, 2000; Liu *et al.*, 2001). It should be noted that in our experiments, the Hill-coefficient of the sigmoidal fit for Ba<sup>2+</sup> block in HPASM cells was shallow. The most logical explanation is that whole-cell current contains at least 2 populations of K<sub>IR</sub> channels with different Ba<sup>2+</sup> sensitivities. Indeed if our data were fitted with a double exponential using slope values obtained from cloned Kir2.1 and Kir2.4, this would give rise to a highly Ba<sup>2+</sup> sensitive component contributing about 25% of the total current with the remainder showing a much lower Ba<sup>2+</sup> sensitivity (not shown). Heteromultimerisation of Kir2.1 and Kir2.4 is also unlikely to explain our data since co-expressing these subunits or a tandem construct, resulted not only in currents exhibiting a greater sensitivity to Ba<sup>2+</sup> compared to Kir2.1 alone but a Hill co-efficient of the Ba<sup>2+</sup> block close to 1 (Schram *et al.*, 2002). The possibility that Kir2.2 contributes to the highly Ba<sup>2+</sup>-sensitive component, however, still remains.

### Single channel properties of K<sub>IR</sub> channels

Few single channel recordings of K<sub>IR</sub> channels have been reported, and none to our knowledge in vascular smooth muscle. We successfully recorded single channel currents corresponding to K<sub>IR</sub> channels in HPASM cells having single channel conductances ranging from 7 to 35 pS, with the majority having conductances in the region of 17 to 22 pS. In heterologous expression systems, single channel conductances for Kir2.1, 2.2, 2.3 and 2.4 have been reported to be around 20 pS, 35 pS, 10 pS and 15 pS, respectively in symmetrical 140 mM K<sup>+</sup> (Topert *et al.*, 1998; Nichols & Lopatin, 1997). In guinea-pig ventricular myocytes, at least 3 types of K<sub>IR</sub> channels have been reported with mean conductance values of 34.0, 23.8 and 10.7 pS, corresponding most likely to Kir2.2, Kir2.1 and Kir2.3, respectively (Liu *et al.*, 2001). In cultured bovine pulmonary artery endothelial cells, a single channel conductance of 31 pS was reported in symmetrical 150 mM K<sup>+</sup> (Kamouchi *et al.*, 1997). Kir2.1 was suggested to underlie this channel, since molecular data provided no evidence for the existence of Kir2.2. The situation appears somewhat different in human aortic endothelial cells, where unitary conductance distributions showed two prominent peaks around 25 and 35 pS with the former peak disappearing in the presence of a Kir2.1 dominant negative construct (Fang *et al.*, 2005). So far, the only single channel data in smooth muscle reports a conductance of 17pS in cells from human small bronchioles (Snetkov & Ward, 1999) which could correspond to either Kir2.1 or Kir2.4. Likewise we measured conductances of 20 pS for Kir2.1 and 19 pS for Kir 2.4 suggesting that K<sub>IR</sub> channels in HPASM cells could correspond to either subunit. It is also worth noting that the presence of Kir2.4 channels could be overlooked in native cells because distinct channel closures were rare unless Ba<sup>2+</sup> was present in the pipette (see also Topert *et al.*, 1998).



Given the low percentage of patches containing  $K_{IR}$  channels in smooth muscle, this could make it difficult to assess the role of Kir2.4, at least at the single channel level.

### Molecular identity of $K_{IR}$ channels in smooth muscle

So far the majority of  $K_{IR}$  currents described in smooth muscle are likely to be composed of Kir2.1 subunits. Consistent with this, RT-PCR analysis of mRNA show transcripts for Kir2.1, but not Kir2.2 or Kir2.3, in rat cerebral, mesenteric and coronary artery (Bradley *et al.*, 1999), canine colon (Flynn *et al.*, 1999) and bronchial smooth muscle (Oonuma *et al.*, 2002). In cultured human bronchial cells,  $K_{IR}$  currents were suppressed by ~75 % with antisense oligonucleotides targeted to Kir2.1 mRNA. While such evidence points to major role of Kir2.1, the expression of Kir2.4 was not examined in these studies. In contrast, immunostaining of rat lung sections identified a high level of Kir2.1 expression in arterial and venous endothelial cells but little to none in the smooth muscle layer (Michelakis *et al.*, 2001; Hogg *et al.*, 2002). Interestingly, heterogeneous expression of Kir2.1 was found in the circular muscle layer of the colon, which was associated with a biphasic and differential sensitivity of  $Ba^{2+}$  on electrical activity (Flynn *et al.*, 1999). This strongly suggests the existence of more than one  $K_{IR}$  conductance; Kir2.4 might be a good candidate since high micromolar  $Ba^{2+}$  was required to observe substantial depolarisation.

In cultured HPASM cells we found message for Kir2.1, Kir2.2 and Kir2.4, suggesting whole-cell currents could be made up of a combination of different subunits. Indeed, co-expression of different members of Kir2.0 subfamily has previously been demonstrated in various tissues. For instance, real-time PCR in rat aortic tissue and human aortic endothelial cells showed that Kir2.2 was the prominent species expressed, followed by Kir2.4 (Alioua *et al.*, 2003; Fang *et al.*, 2005). Kir2.3 and 2.1 were also present, but were less abundant. Furthermore, Kir2.1, Kir2.2 and Kir2.3 were all detected by immunostaining in rat CA1-CA3 pyramidal neurons, granule layer cells of the hippocampus and in rat middle cerebral arteries (Stonehouse *et al.*, 1999). In cardiac myocytes, both Kir2.1 and Kir2.2 appear critical components of native  $K_{IR}$  current ( $IK_1$ ), though the relative subunit contribution appears to change from neonatal to adult heart (Nakamura *et al.*, 1999; Liu *et al.*, 2001; Zaritsky *et al.*, 2001). Thus, the expression of multiple Kir2.0 subunits appears a widespread finding.

### Functional role of $K_{IR}$ channels

$K_{IR}$  channels have been suggested to play an important role in maintaining the resting membrane potential and involved in the  $K^+$ -induced hyperpolarization of vascular smooth muscle (Edwards *et al.*, 1988; Knot *et al.*, 1996; Quayle *et al.*, 1996; Quayle *et al.*, 1997). In some vessels,  $K_{IR}$  channels are the target for endothelium-derived hyperpolarising factor (EDHF) where  $K^+$ , liberated *via* endothelial  $Ca^{2+}$ -sensitive  $K^+$  channels, is thought to activate  $K_{IR}$  channels within the smooth muscle layer (Edwards & Weston, 2004). These channels also appear to underlie relaxation to the stable prostacyclin analogue, cicaprost in rat tail artery (Orie *et al.*, 2006). Genetic manipulation has been employed recently to further clarify the molecular nature of  $K_{IR}$  channels and their function in smooth muscle. Using Kir2.1 and Kir2.2 knock-out mice, the presence of  $K_{IR}$  currents was observed in cerebral artery smooth muscle cells isolated from control animals but were absent in myocytes from Kir2.1<sup>-/-</sup> animals (Zaritsky *et al.*, 2000). In addition, the dilator response to  $K^+$  was completely absent in Kir2.1<sup>-/-</sup> but not Kir2.2<sup>-/-</sup> animals, suggesting the functional importance of Kir2.1 (Zaritsky *et al.*, 2000). Our data showing  $Ba^{2+}$  (100  $\mu$ M) to significantly depolarize the resting membrane potential in cultured HPASM cells suggests that  $K_{IR}$  channels do indeed contribute to the resting membrane potential in these cells. The relatively high  $Ba^{2+}$  required, may point to significant role for Kir2.4. Interestingly, we found that Kir2.4 passed significantly more outward current compared to Kir2.1, making it a

good candidate to regulate the resting potential in those tissues expressing Kir2.4. However, in view of the fact that changes in gene expression may well occur in culture and alter the electrophysiological properties of HPASM cells (Cui et al., 2002), it remains to be determined whether Kir2.4 contributes to  $K_{IR}$  currents in the pulmonary vasculature *in vivo*.

## Acknowledgments

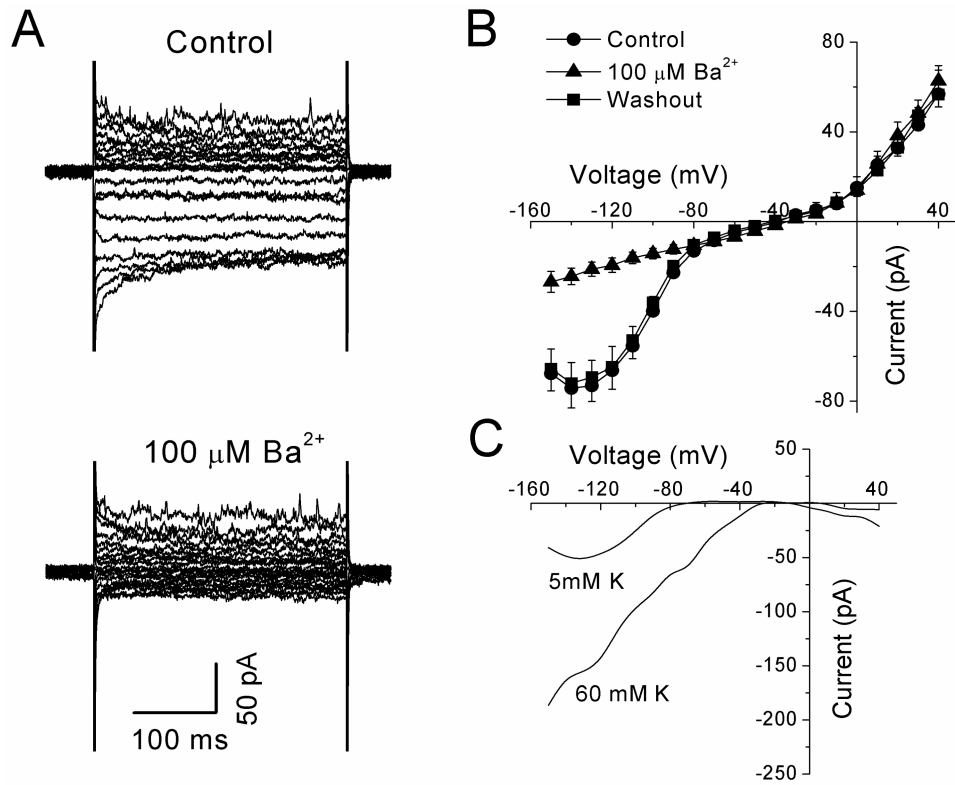
This work was supported by the British Heart Foundation (PG 99176 & PG/03/062). LHC is an MRC Senior Fellow in Basic Science (G117/440).

## REFERENCES

- Alioua A, Conti L, Eghbali M, Mahajan A, Tanaka Y, Stefani E, Vandenberg C, Toro L. Inward rectifier  $K^+$  channels (Kir) control muscle tone of a rat conduit vessel: Role of Kir2.x. *Biophys. J.* 2003; 84:225A.
- Bradley KK, Jaggar JH, Bonev AD, Heppner TJ, Flynn ERM, Nelson MT, Horowitz B.  $K_{IR}2.1$  encodes the inward rectifier potassium channel in rat arterial smooth muscle. *J. Physiol. (London)*. 1999; 515:639–651. [PubMed: 10066894]
- Cui Y, Giblin JP, Clapp LH, Tinker A. A mechanism for ATP-sensitive potassium channel diversity: functional coassembly of two pore forming subunits. *Proc. Natl. Acad. Sci. U. S. A.* 2001; 98:729–734. [PubMed: 11136227]
- Cui Y, Tran S, Tinker A, Clapp LH. The molecular composition of  $K_{ATP}$  channels in human pulmonary artery smooth muscle cells and their modulation by growth. *Am. J. Respir. Cell. Molec. Biol.* 2002; 26:135–143. [PubMed: 11751213]
- Edwards FR, Hirst GDS, Silverberg GD. Inward rectification in rat cerebral arterioles: Involvement of potassium ions in autoregulation. *J. Physiol. (London)*. 1988; 404:455–466. [PubMed: 3253438]
- Edwards G, Weston AH. Potassium and potassium currents in endothelium-dependent hyperpolarizations. *Pharmacol. Res.* 2004; 49:535–541. [PubMed: 15026031]
- Fang Y, Schram G, Romanenko VG, Shi C, Conti L, Vandenberg CA, Davies PF, Nattel S, Levitan I. Functional expression of Kir2.x in human aortic endothelial cells: the dominant role of Kir2.2. *Am. J. Physiol.* 2005; 289:C1134–C1144. [PubMed: 15958527]
- Flynn ERM, McManus CA, Bradley KK, Koh SD, Hegarty TM, Horowitz B, Sanders KM. Inward rectifier potassium conductance regulates membrane potential of canine smooth muscle. *J. Physiol. (London)*. 1999; 518:247–256. [PubMed: 10373706]
- Giblin JP, Leaney JL, Tinker A. The molecular assembly of ATP-sensitive potassium channels: Determinants on the pore forming subunit. *J. Biol. Chem.* 1999; 274:22652–22659. [PubMed: 10428846]
- Hoger JH, Ilyin VI, Forsyth S, Hoger A. Shear stress regulates the endothelial Kir2.1 ion channel. *Proc. Natl. Acad. Sci. U. S. A.* 2002; 99:7780–7785. [PubMed: 12032360]
- Hogg DS, McMurray G, Kozlowski RZ. Endothelial cells freshly isolated from small pulmonary arteries of the rat possess multiple distinct  $K^+$  current profiles. *Lung*. 2002; 180:203–214. [PubMed: 12391510]
- Hughes BA, Kumar G, Yuan Y, Swaminathan A, Yan D, Sharma A, Plumley L, Yang-Feng TL, Swaroop A. Cloning and functional expression of human retinal Kir2.4, a pH-sensitive inwardly rectifying  $K^+$  channel. *Am. J. Physiol.* 2000; 279:C771–C784. [PubMed: 10942728]
- Kamouchi M, Van Den Bremt K, Eggermont J, Droogmans G, Nilius B. Modulation of inwardly rectifying potassium channels in cultured bovine pulmonary artery endothelial cells. *J. Physiol. (London)*. 1997; 504:545–556. [PubMed: 9401963]
- Knot HJ, Zimmermann PA, Nelson MT. External  $K^+$  induced dilations of rat coronary and cerebral arteries involve inward rectifier  $K^+$  channels. *J. Physiol. (London)*. 1996; 492:419–430. [PubMed: 9019539]
- Liu GX, Derst C, Schlichthorl G, Heinen S, Seeböhm G, Bruggemann A, Kummer W, Veh RW, Daut J, Preisig-Müller R. Comparison of cloned Kir2 channels with native inward rectifier  $K^+$  channels from guinea-pig cardiomyocytes. *J. Physiol. (London)*. 2001; 532:115–126. [PubMed: 11283229]

- Michelakis ED, Weir EK, Wu X, Nsair A, Waite R, Hashimoto K, Puttagunta L, Knaus HG, Archer SL. Potassium channels regulate tone in rat pulmonary veins. *Am. J. Physiol.* 2001; 280:L1138–L1147. [PubMed: 11350792]
- Nakamura TY, Lee K, Artman M, Rudy B, Coetzee WA. The role of Kir2.1 in the genesis of native cardiac inward-rectifier K<sup>+</sup> currents during pre- and postnatal development. *Ann. N. Y. Acad. Sci.* 1999; 868:434–437. [PubMed: 10414316]
- Nichols CG, Lopatin AN. Inward rectifier potassium channels. *Annu. Rev. Physiol.* 1997; 59:171–191. [PubMed: 9074760]
- Nilius B, Droogmans G. Ion channels in the vascular endothelium. *Physiol. Rev.* 2001; 81:1415–1459. [PubMed: 11581493]
- Oonuma H, Iwasawa K, Iida H, Nagata T, Imuta H, Morita Y, Yamamoto K, Nagai R, Omata M, Nakajima T. Inward rectifier K<sup>+</sup> current in human bronchial smooth muscle cells: inhibition with antisense oligonucleotides targeted to Kir2.1 mRNA. *Am. J. Respir. Cell Mol. Biol.* 2002; 26:371–379. [PubMed: 11867346]
- Orie NN, Fry CH, Clapp LH. Evidence that inward rectifier K<sup>+</sup> channels mediate relaxation by the PGI<sub>2</sub> receptor agonist cicaprost via a cyclic AMP-independent mechanism. *Cardiovasc. Res.* 2006; 69:107–115. [PubMed: 16183044]
- Preisig-Muller R, Schlichthorl G, Goerge T, Heinen S, Bruggemann A, Rajan S, Derst C, Veh RW, Daut J. Heteromerization of Kir2.x potassium channels contributes to the phenotype of the Andersen's syndrome. *Proc. Natl. Acad. Sci. U. S. A.* 2002; 99:7774–7779. [PubMed: 12032359]
- Quayle JM, Dart C, Standen NB. The properties and distribution of inward rectifier potassium currents in pig coronary arterial smooth muscle. *J. Physiol. (London).* 1996; 494:715–726. [PubMed: 8865069]
- Quayle JM, Mccarron JG, Brayden JE, Nelson MT. Inward rectifier K<sup>+</sup> currents in smooth muscle cells from rat resistance-sized cerebral arteries. *Am. J. Physiol.* 1993; 265:C1363–C1370. [PubMed: 7694496]
- Quayle JM, Nelson MT, Standen NB. ATP-sensitive and inwardly rectifying potassium channels in smooth muscle. *Physiol. Rev.* 1997; 77:1166–1232. [PubMed: 9354814]
- Robertson BE, Bonev AD, Nelson MT. Inward rectifier K<sup>+</sup> currents in smooth muscle cells from rat coronary arteries: Block by Mg<sup>2+</sup>, Ca<sup>2+</sup>, and Ba<sup>2+</sup>. *Am. J. Physiol.* 1996; 40:H696–H705. [PubMed: 8770113]
- Sakai H, Shimizu T, Hori K, Ikari A, Asano S, Takeguchi N. Molecular and pharmacological properties of inwardly rectifying K<sup>+</sup> channels of human lung cancer cells. *Eur. J. Pharmacol.* 2002; 435:125–133. [PubMed: 11821018]
- Schram G, Melnyk P, Pourrier M, Wang Z, Nattel S. Kir2.4 and Kir2.1 K<sup>+</sup> channel subunits co-assemble: a potential new contributor to inward rectifier current heterogeneity. *J. Physiol.* 2002; 544:337–349. [PubMed: 12381809]
- Shimoda LA, Welsh LE, Pearse DB. Inhibition of inwardly rectifying K<sup>+</sup> channels by cGMP in pulmonary vascular endothelial cells. *Am. J. Physiol.* 2002; 283:L297–L304. [PubMed: 12114190]
- Snetkov VA, Ward JPT. Ion currents in smooth muscle cells from human small bronchioles: presence of an inward rectifier K<sup>+</sup> current and three types of large conductance K<sup>+</sup> channels. *Exp. Physiol.* 1999; 84:835–846. [PubMed: 10502653]
- Stanfield PR, Nakajima S, Nakajima Y. Constitutively active and G-protein coupled inward rectifier K<sup>+</sup> channels: Kir2.0 and Kir3.0. *Rev. Physiol Biochem. Pharmacol.* 2002; 145:47–179. [PubMed: 12224528]
- Stonehouse AH, Pringle JH, Norman RI, Stanfield PR, Conley EC, Brammar WJ. Characterisation of Kir2.0 proteins in the rat cerebellum and hippocampus by polyclonal antibodies. *Histochem. Cell Biol.* 1999; 112:457–465. [PubMed: 10651097]
- Topert C, Doring F, Wischmeyer E, Karschin C, Brockhaus J, Ballanyi K, Derst C, Karschin A. Kir2.4: a novel K<sup>+</sup> inward rectifier channel associated with motoneurons of cranial nerve nuclei. *J. Neurosci.* 1998; 18:4096–4105. [PubMed: 9592090]

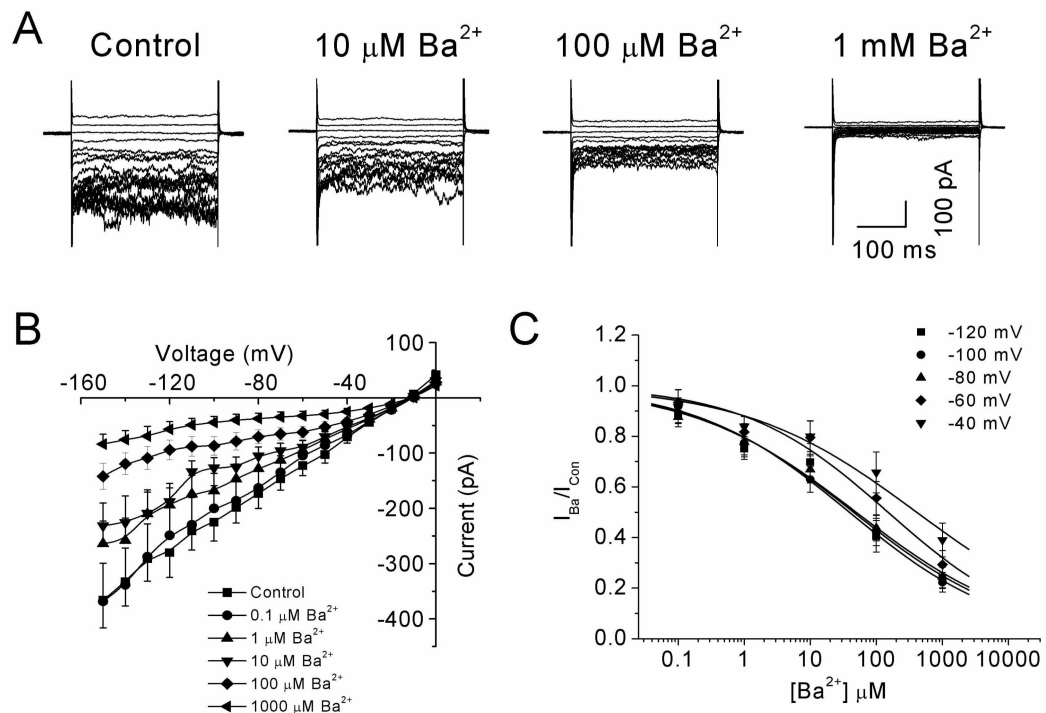
- Voets T, Droogmans G, Nilius B. Membrane currents and the resting membrane potential in cultured bovine pulmonary artery endothelial cells. *J. Physiol. (London)*. 1996; 497:95–107. [PubMed: 8951714]
- Woodhull AM. Ionic blockage of sodium channels in nerve. *J. Gen. Physiol.* 1973; 61:687–708. [PubMed: 4541078]
- Zaritsky JJ, Eckman DM, Wellman GC, Nelson MT, Schwarz TL. Targeted disruption of Kir2.1 and Kir2.2 genes reveals the essential role of the inwardly rectifying K<sup>+</sup> current in K<sup>+</sup>-mediated vasodilation. *Circ. Res.* 2000; 87:160–166. [PubMed: 10904001]
- Zaritsky JJ, Redell JB, Tempel BL, Schwarz TL. The consequences of disrupting cardiac inwardly rectifying K<sup>+</sup> current (I<sub>K1</sub>) as revealed by the targeted deletion of the murine Kir2.1 and Kir2.2 genes. *J. Physiol. (London)*. 2001; 533:697–710. [PubMed: 11410627]



**Figure 1.**

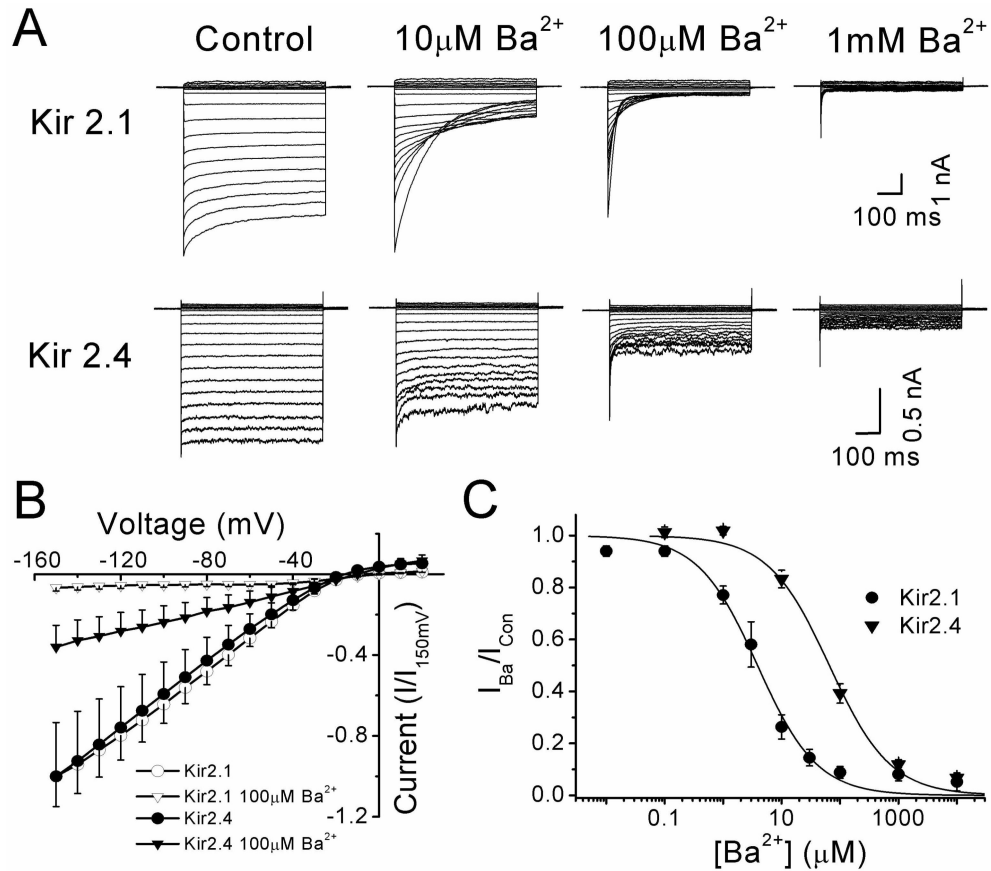
(A) Effects of Ba<sup>2+</sup> (100 μM) on currents evoked by 300 ms voltage steps from -150 mV to +40 mV at a holding potential of -60 mV in a single HPASM cell. (B) Mean I-V curves obtained from a series of experiments (n=8) similar to above, obtained under control conditions, in the presence of Ba<sup>2+</sup> and following washout. (C) I-V curves of Ba<sup>2+</sup>-sensitive currents recorded in physiological K<sup>+</sup> (5/140 mM) and high (60/140 mM) K<sup>+</sup> gradients. Data is expressed as mean ± S.E.M.



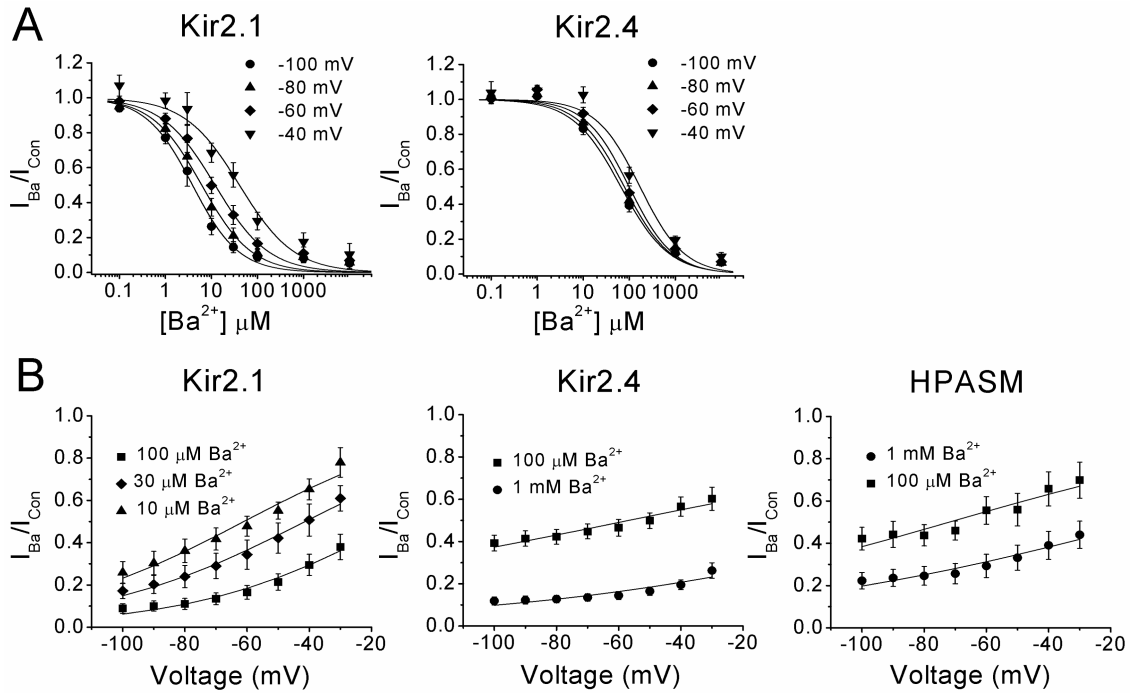


**Figure 2.**

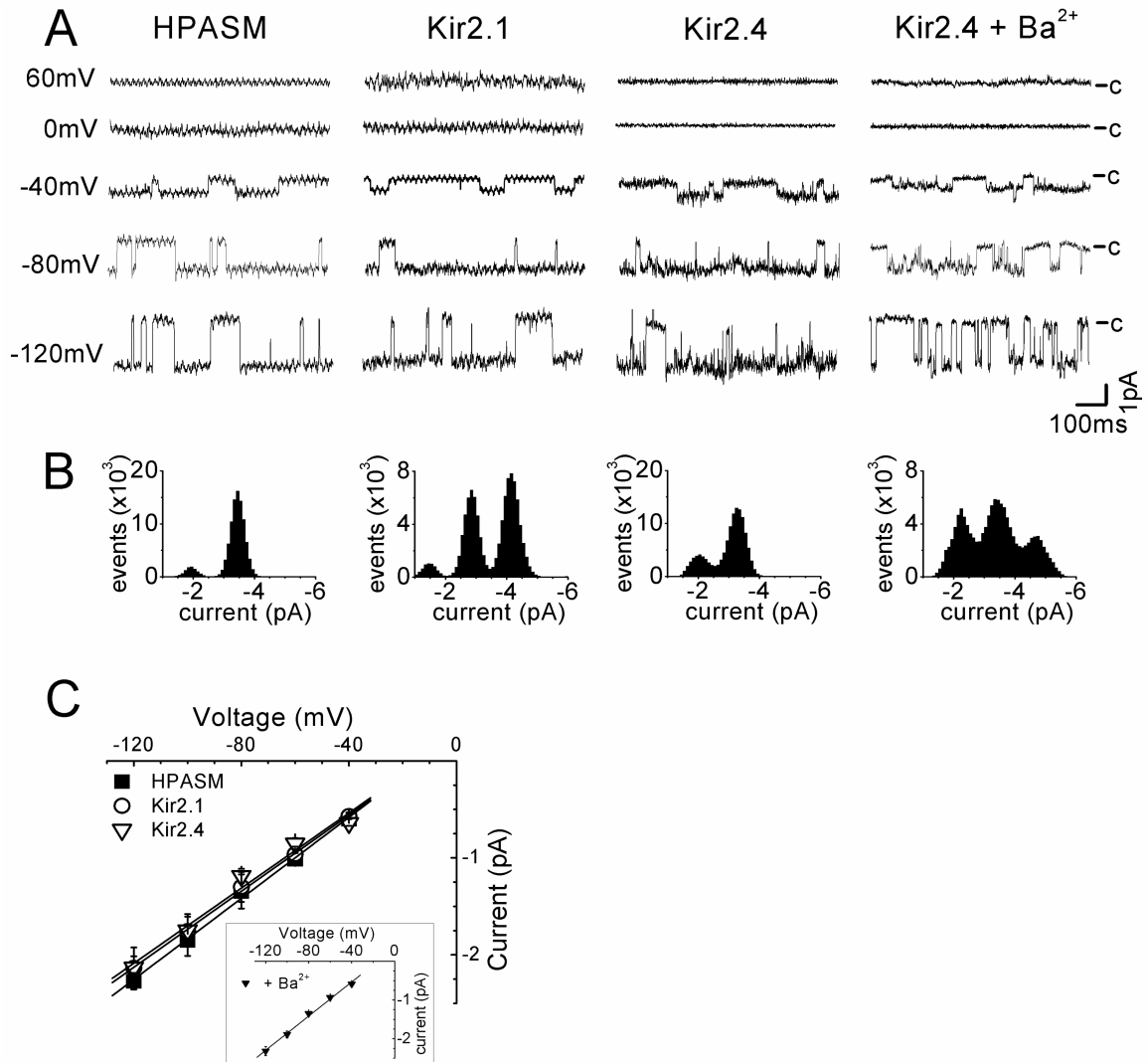
Concentration-dependence of the  $\text{Ba}^{2+}$  block of  $\text{K}_{\text{IR}}$  currents in HPASM cells. (A) Effects of  $\text{Ba}^{2+}$  on a family of currents evoked by 300 ms voltage steps from  $-150$  to  $0$  mV at a holding potential of  $-20$  mV. (B) Mean I-V relationships of steady-state current recorded in the absence and presence of increasing concentrations of  $\text{Ba}^{2+}$  ( $n=9$ ). (C) Concentration-response curves for the  $\text{Ba}^{2+}$ -induced block measured at various potentials ( $-120$  to  $-40$  mV). The solid lines represent best fit of the data to Eq. 1. Values for the  $\text{IC}_{50}$  and the slope factor ( $n$ ) were  $45.2$   $\mu\text{M}$  ( $n=0.36$ ),  $39.1$   $\mu\text{M}$  ( $n=0.37$ ),  $49.4$   $\mu\text{M}$  ( $n=0.35$ ),  $150.0$   $\mu\text{M}$  ( $n=0.40$ ) and  $407.6$   $\mu\text{M}$  ( $n=0.33$ ) at  $-120$  mV,  $-100$  mV,  $-80$  mV,  $-60$  mV and  $-40$  mV, respectively.

**Figure 3.**

Whole-cell characteristics of Kir2.1 and Kir2.4 stably expressed in HEK 293 cells showing differential sensitivity to  $\text{Ba}^{2+}$ . (A) Effects of increasing concentration of  $\text{Ba}^{2+}$  on a family of currents evoked by 600 ms voltage steps from  $-150$  to  $+20$  mV at a holding potential of  $-20$  mV in a 60/140  $\text{K}^+$  gradient. (B) Mean I-V relationships of steady-state current plotted relative to control current at  $-150$  mV recorded in the absence (○) and presence (▼) of 100  $\mu\text{M}$   $\text{Ba}^{2+}$  for currents expressed by Kir2.1 ( $n=6-12$ ) (closed symbols) and Kir2.4 ( $n=6$ ) (open symbols). (C) Concentration-response curves for the  $\text{Ba}^{2+}$ -induced block shown for currents recorded at  $-100$  mV. Values for the dissociation constant ( $K_D$ ) and the slope factor ( $n$ ) were derived by the fit to Eq 1. For Kir 2.1, the  $K_D$  was  $3.9\ \mu\text{M}$  ( $n=0.85$ ) at  $-100$  mV, and the corresponding value for Kir 2.4 was  $65.6\ \mu\text{M}$  ( $n=0.83$ )

**Figure 4.**

Voltage-dependence of the  $Ba^{2+}$ -induced block in cells expressing Kir2.1 or Kir2.4 compared with endogenous  $K_{IR}$  currents expressed in HPASM cells. (A) Concentration-response curves for the  $Ba^{2+}$ -induced block of inward currents activated at various potentials from -100 to -40 mV by Kir2.1 and Kir2.4. The solid lines represent best fits of data to Eq. 1. Stepping from a potential of -100 mV to -40 mV, the  $K_D$  increased from 3.9  $\mu M$  to 40.6  $\mu M$  for Kir2.1 and 65.6  $\mu M$  to 170.5  $\mu M$  for Kir2.4. (B) The voltage-dependence of the block was assessed by plotting the fractional block against membrane potential at a single  $Ba^{2+}$  concentration for Kir2.1, Kir2.4 and HPASM cells. Solid lines are the best fit of Eq. 2. The parameters at a blocking concentration of 100  $\mu M$   $Ba^{2+}$  were  $K_D(0) = 142 \pm 23 \mu M$ ,  $197 \pm 18 \mu M$ ,  $337 \pm 45 \mu M$  and  $\delta = 0.38 \pm 0.04$ ,  $0.15 \pm 0.02$ ,  $0.21 \pm 0.03$ , for Kir2.1 (n=10), Kir2.4 (n=9) and HPASM (n=9) cells, respectively. At 1 mM  $Ba^{2+}$ ,  $K_D(0)$  values were  $411.3 \pm 89.9$  and  $1142 \pm 161 \mu M$  and  $\delta$  values were  $0.15 \pm 0.04$  and  $0.19 \pm 0.06$ , for Kir2.4 and HPASM, respectively. All data are expressed as mean  $\pm$  S.E.M.

**Figure 5.**

Single channel analysis of  $K_{IR}$  channels. (A) Single unitary events recorded in the cell-attached configuration from a HAPSM cell and HEK293 cells expressing either Kir2.1 or Kir2.4. Currents, filtered at 500 Hz, were recorded at various test potentials from  $-120$  to  $+60$  mV in symmetrical 140/140 mM  $K^+$ , with the closed state indicated. Due to the low frequency of closings with Kir2.4 channels, recordings were also made in the presence of 300  $\mu$ M  $BaCl_2$  in the patch pipette. (B) All points amplitude histograms for recordings shown in (A) at a test potential of  $-80$  mV for identical 20 s recordings (0.1 pA bin-width). (C) Mean single channel I-V relationships recorded in HPASM cells (closed squares,  $n=6$ ) and HEK293 cells expressing either Kir2.1 (open circles  $n=7$ ) or Kir2.4 (open triangles,  $n=4$ ) with the inset showing recordings in the presence  $BaCl_2$  ( $n=5$ ). Slope conductances were obtained by linear regression giving values of  $20.5 \pm 0.9$  pS,  $19.6 \pm 0.9$  pS,  $19.4 \pm 1.7$  pS,  $22.0 \pm 0.9$  pS, for HPASM, Kir2.1, Kir2.4, and Kir2.4 in the presence of  $Ba^{2+}$ , respectively.

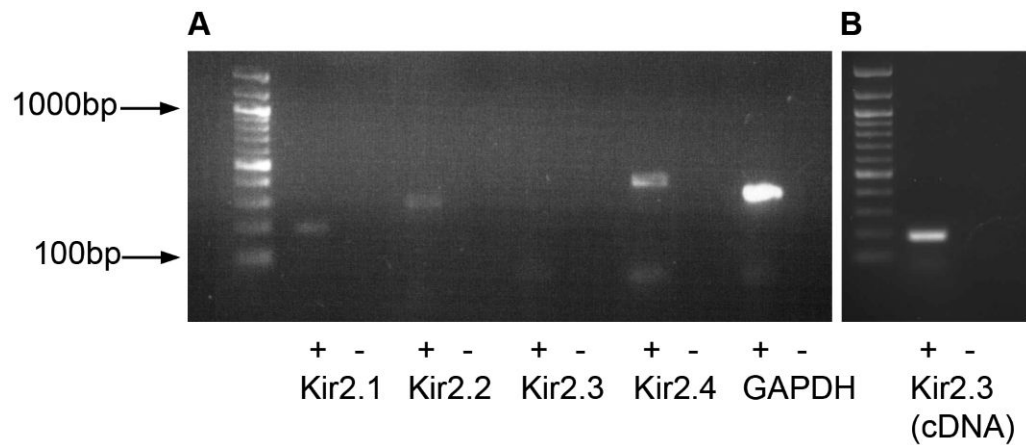


**Figure 6.**

(A) RT-PCR analysis of Kir2.0 subunits in cultured HPASM cells. Lane 1 contains size makers to indicate the size of the PCR products. Visible products were detected for Kir2.1 (lane 2, 199 bp), Kir2.2 (lane 4, 269 bp) and Kir2.4 (lane 8, 378 bp) but not Kir2.3 (lane 6). The reduced form of guanosine adenine dinucleotide phosphate (GAPDH) was used as a positive control for RT-PCT (lane 10). The negative control reactions (absence of reverse transcriptase) were run in lanes 3, 5, 7, and 9. (B) Positive control for Kir2.3. Lane 1 contains size markers, lane 2 contains positive control product for Kir2.3 (178bp) and lane 3 contains reaction with no positive template.